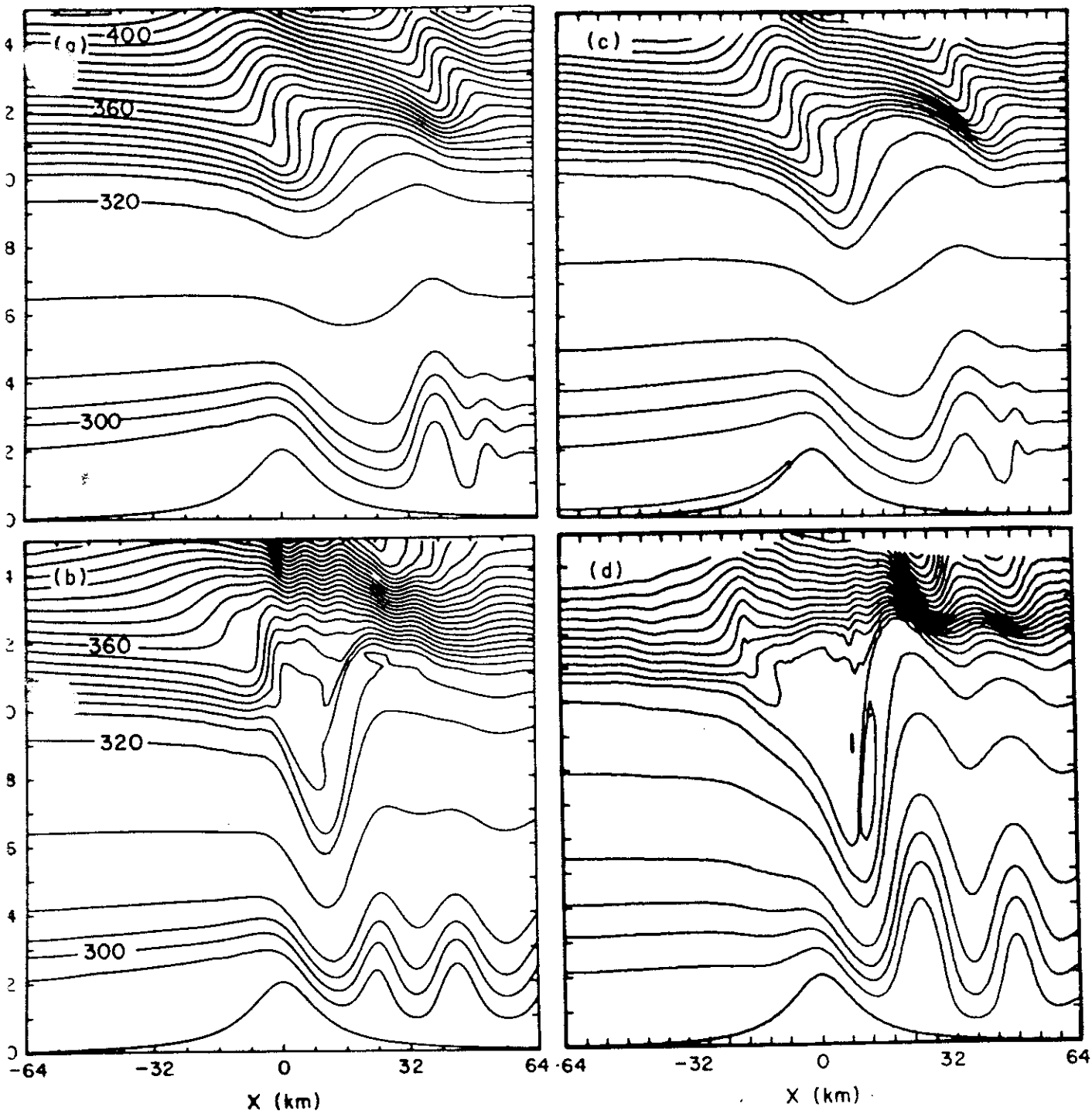


FIG. 11. Isentropes obtained by numerical simulation of the 11 January 1972 Boulder ndstorm using this model at (a) $t$ = 4000 and (b) $t$ = 8000 s. Isentropes determined m the simulation of Peltier and Clark (1979) at (c) $t$ = 4180 and (d) 8000 s. Different tropes are contoured by the different models.

but is gradually amplifying. The not completely steady, and some nerical solution may reflect that

by (42). In the first case discussed in Secti atmosphere was isothermal so that $l$ was ex stant with height. This unrealistic assumpti

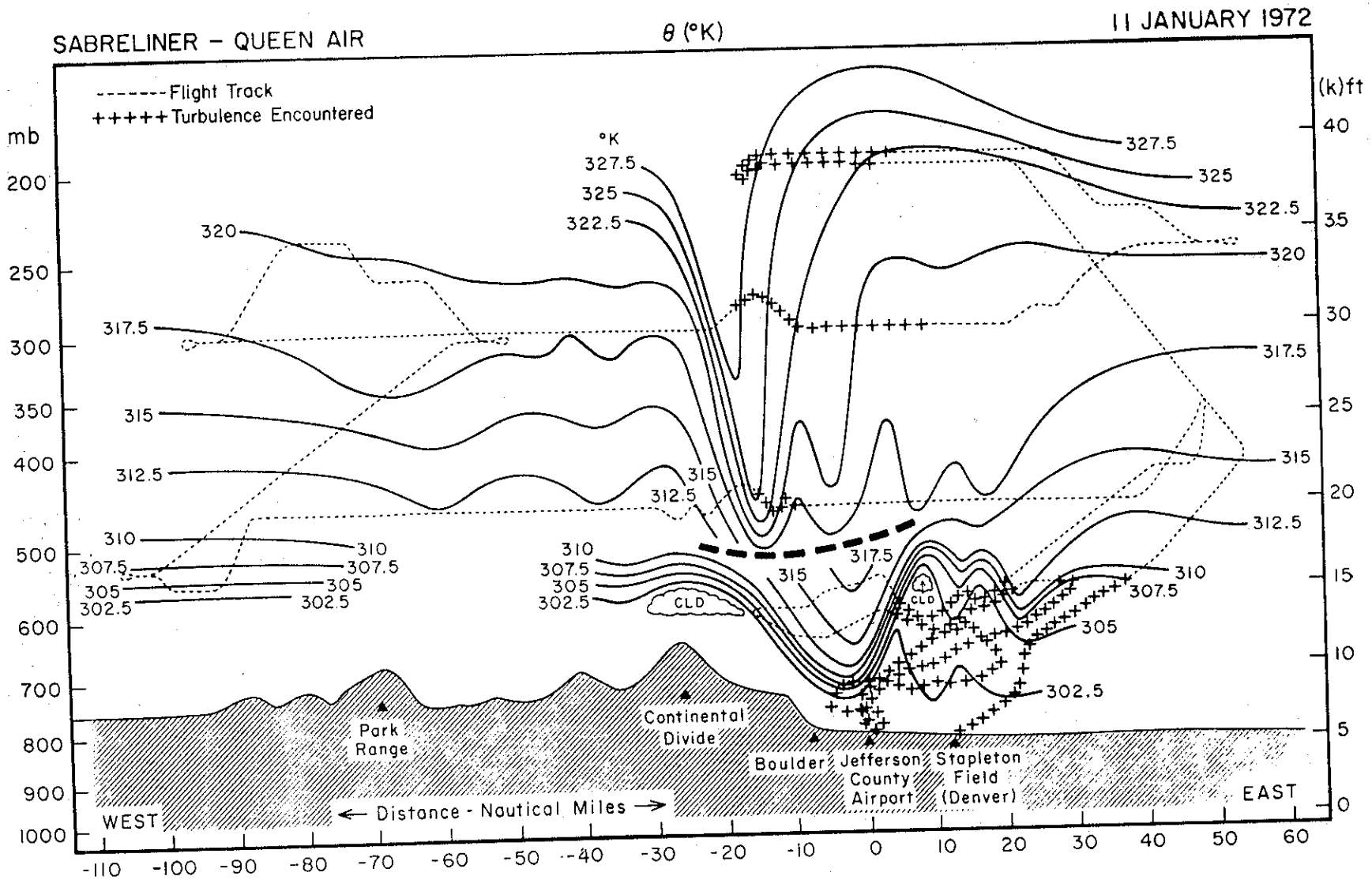


FIG. 7. Analysis of the potential temperature field (solid lines) from aircraft flight data and sondes taken on 11 January 1972. The dashed lines show aircraft track, with periods of significant turbulence shown by pluses. The heavy dashed line separates data taken by the Queen Air at lower levels before 2200 GMT from that taken by the Sabreliner in the middle and upper troposphere after 0000 GMT (12 January). The aircraft flight tracks were made along an approximate 130°–310° azimuth, but the distances shown are along the east-west projection of those tracks.

(dashed). Data taken from 9–12 January 1972. Stippled area indicates time of Sabreliner flight.

the trough of the primary downstream wave. The turbulence generated in that region was then carried by the subsequent updraft to at least 8 km above the

For one especially notable incident, identified with a star on Fig. 10, we were able to acquire the flight recorder traces of vertical acceleration and altitude. We present and discuss this material in Section 5. The analysis to be discussed in the remainder of this section

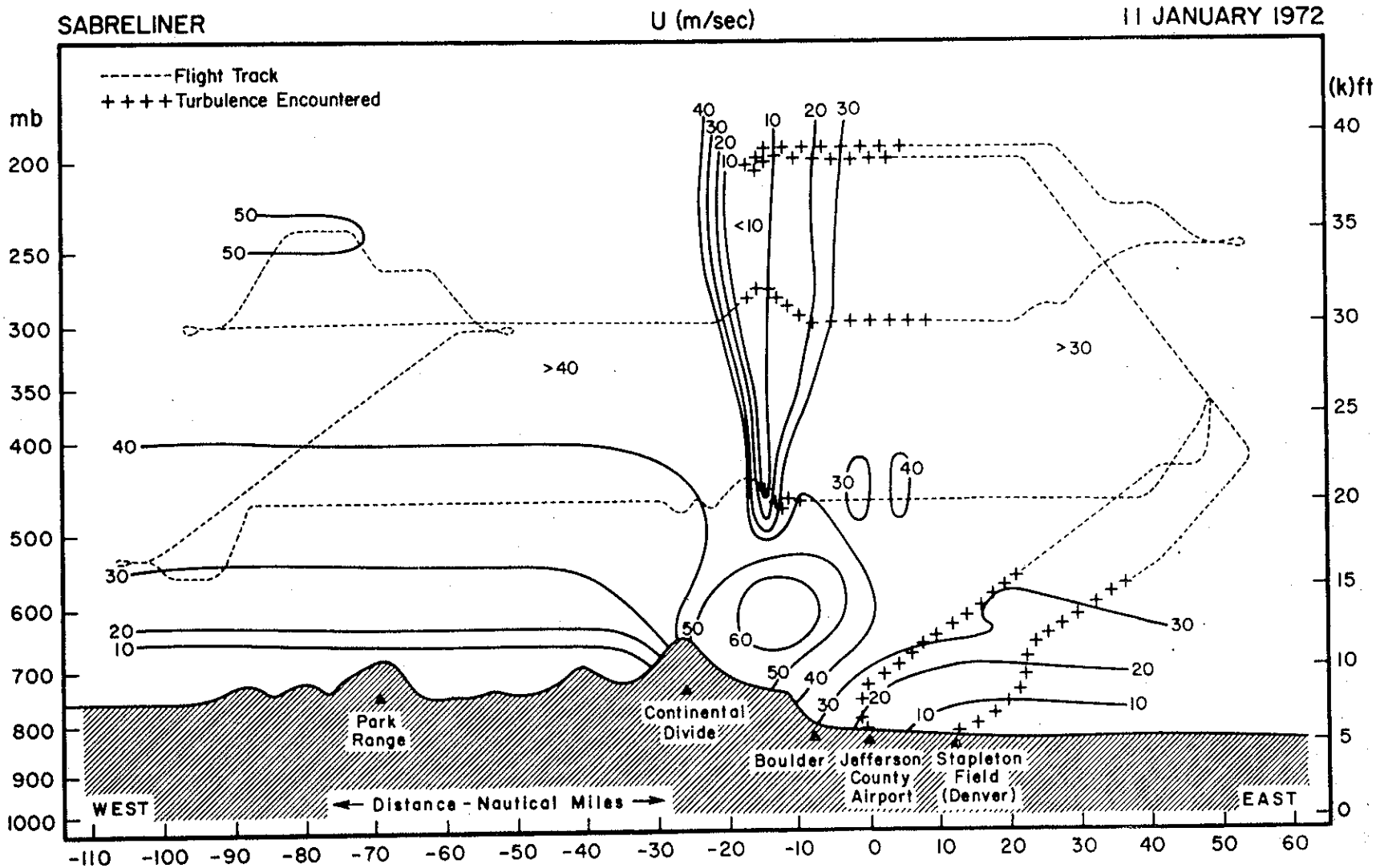


FIG. 9. Analysis of westerly wind component (m $s^{-1}$) on 11 January 1972, made from Sabreliner and sonde data only. The analysis below 470 mb over the eastern slope was deduced from assumptions indicated in the text.

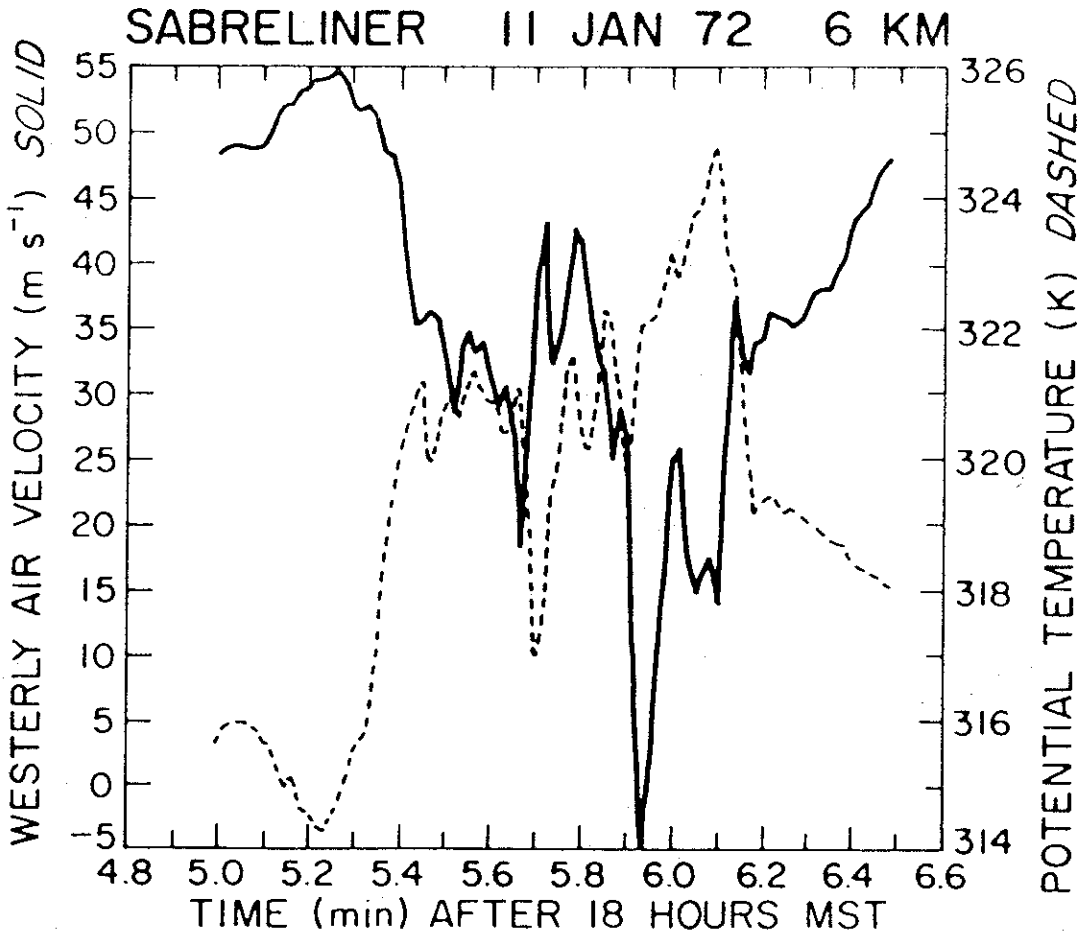


FIG. 13. Westerly velocity (solid) and potential temperature (dashed) in the turbulent zone at 6 km.

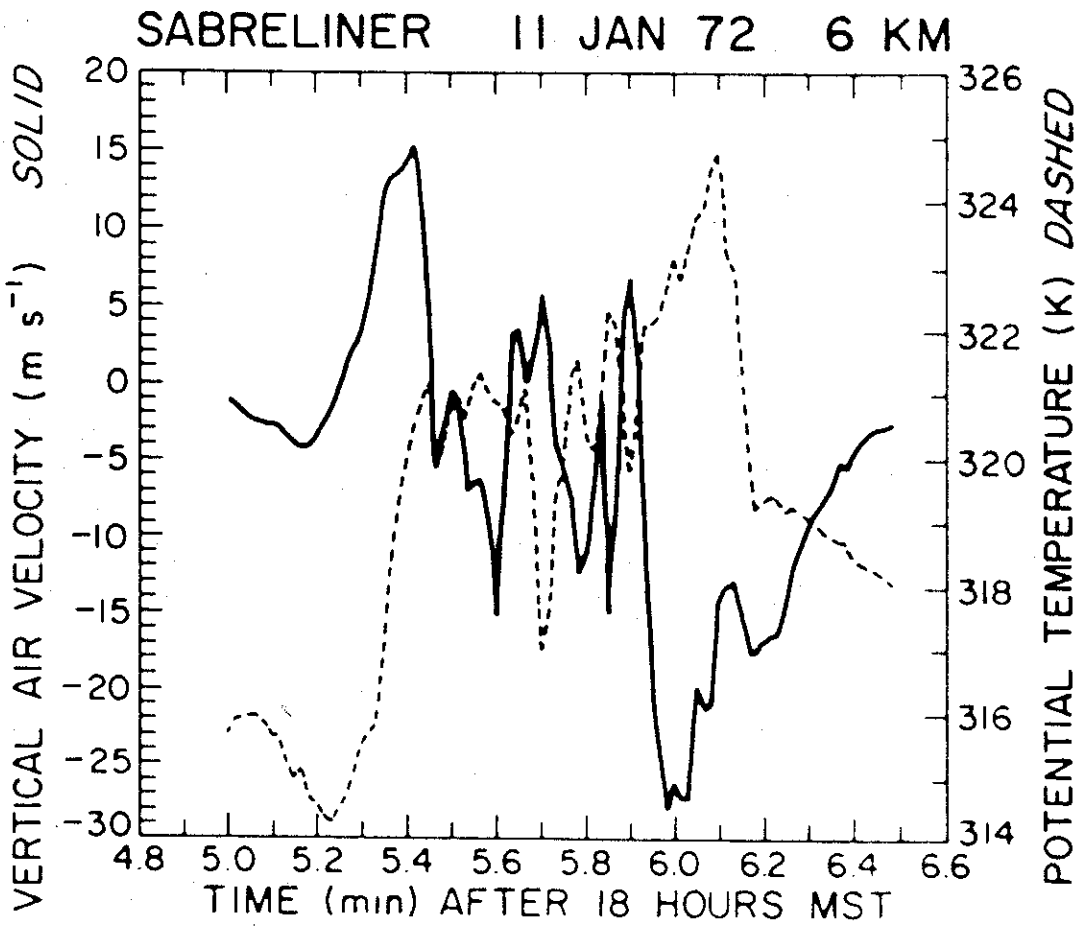


FIG. 12. Vertical velocity (solid) and potential temperature (dashed) in the turbulent zone at 6 km.

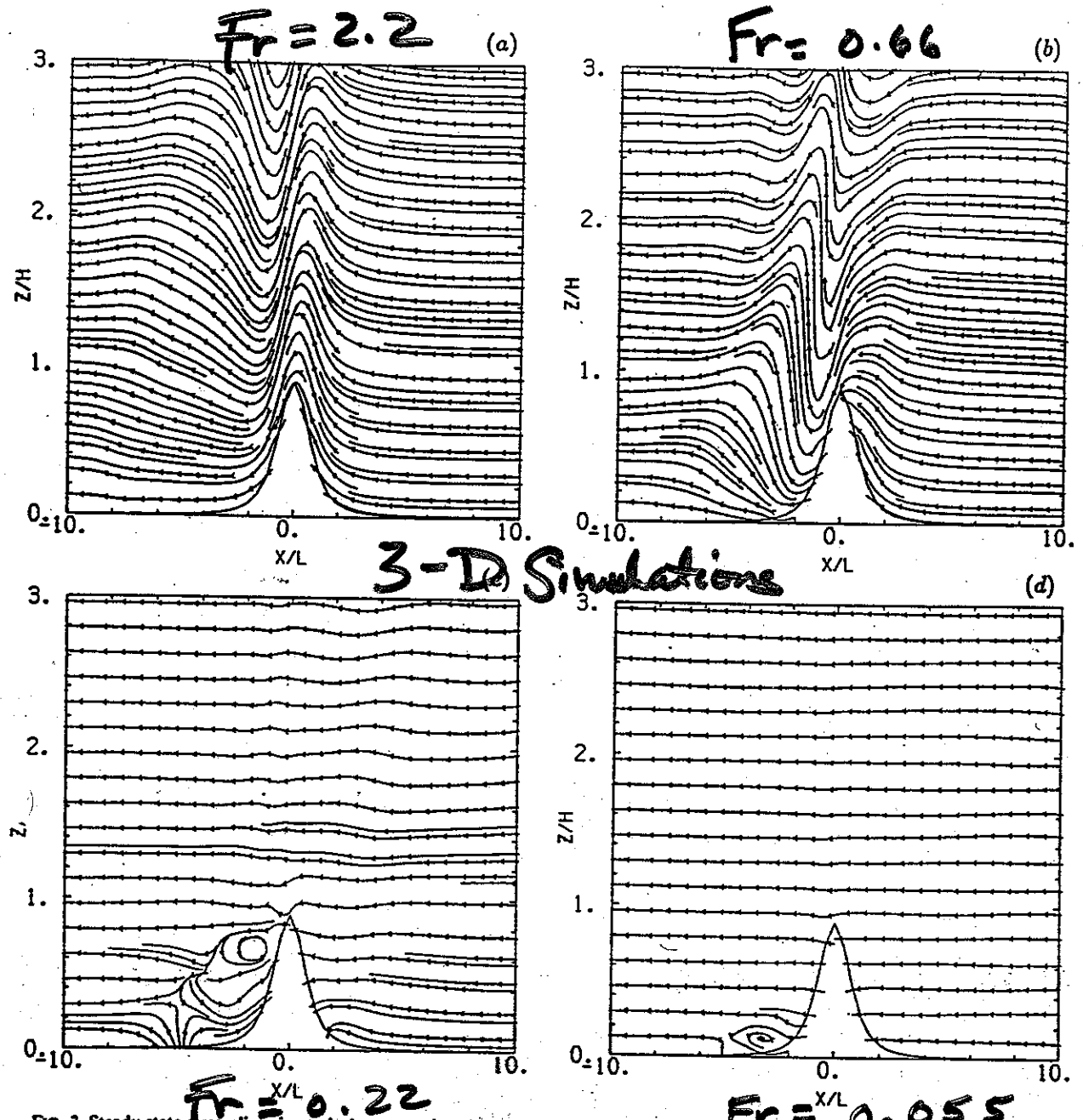


FIG. 3. Steady-state streamlines in vertical cross section through the center plane for Fr = (a) 2.2, (b) 0.66, (c) 0.22, and (d) 0.055.

sured by the maximum value of the nondimensional horizontal velocity in the reversed flow in the lee of the obstacle as a function of Fr. Figure 5b shows the depth of the lee vortices as measured by the height (normalized by $h$) of the reversed flow in the lee of the obstacle as a function of Fr. Both curves exhibit a similar dependence on Fr. These two features remain aproximately constant within the range Fr $\sim$ 0.2–0.4 and decrease rapidly both when Fr $\to$ 0 or Fr $\to$ 0.5. This result is reasonable inasmuch as in the limit Fr $\to$ 0 the solution should approach two-dimensional potential flow, while in the limit Fr $\to \infty$ the solution should approach three-dimensional potential flow; in both limits the vortices should disappear. Figure 5c displays the width of the vortex couplet in the spanwise direction measured by the maximum distance between closed surface streamlines; the shrinking of the vortices with increasing Fr is apparent. Finally, Fig. 5d shows the distance of the vortices from the center of the obstacle measured by the distance of the position of the maximal reversed flow in the lee from the center of the obstacle; as Fr increases the lee vortices approach the

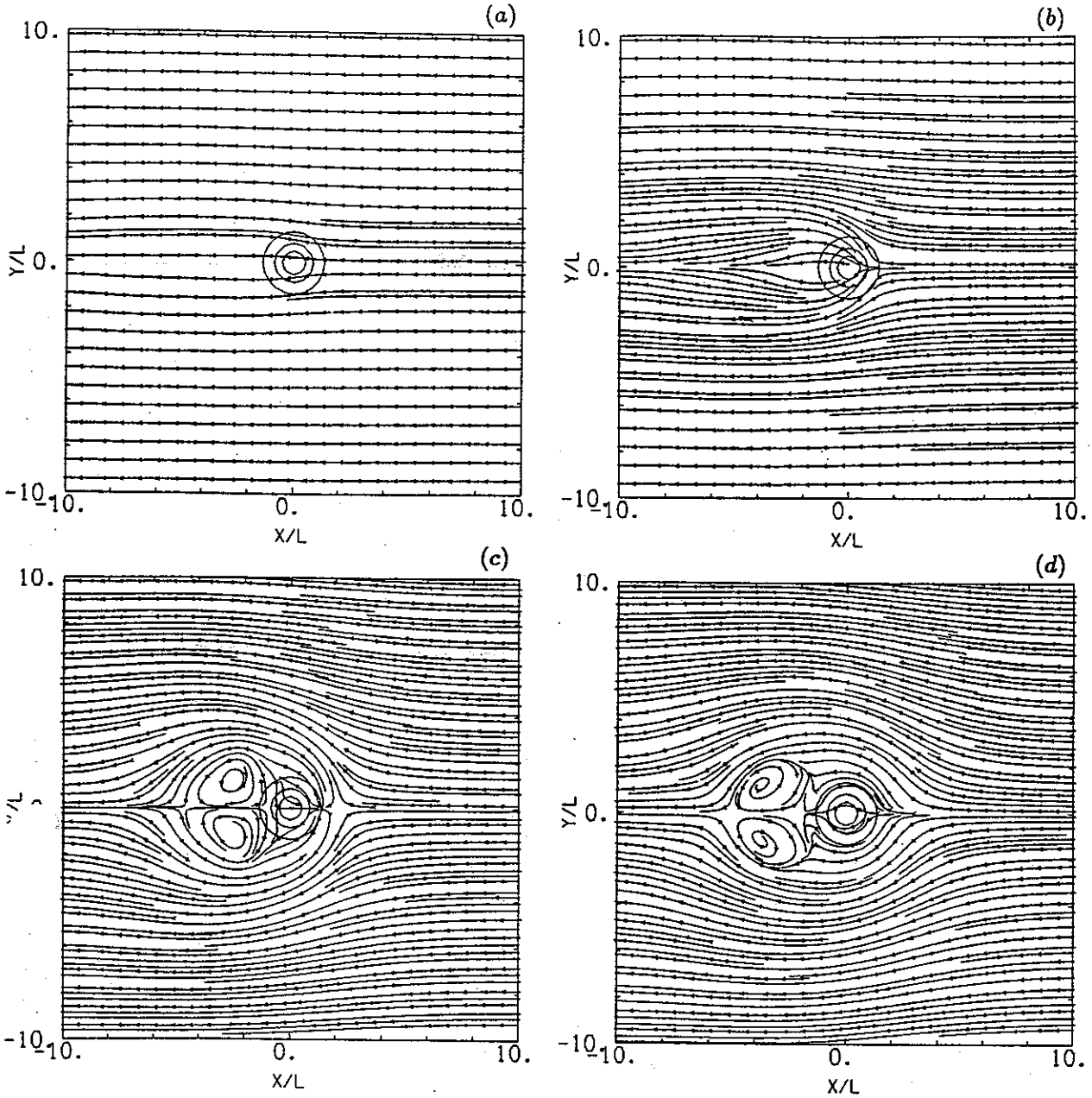


FIG. 1. Steady-state streamlines at the lower surface for Fr = (a) 2.2, (b) 0.66, (c) 0.22, and (d) 0.055. Concentric contours in the center of the domain represent the height of the obstacle with contour interval 0.25 $h$.

valid in this limit. As Fr $\searrow$ 0.5 flow stagnation occurs on the windward and leeward sides and the flow takes a dramatically different form. Whether or not linear theory describes this flow transition as a function of Fr is not clear. What is clear from these experiments is that the lee vortices and the reversal of the low-level, upwind-side flow seem to appear together as Fr $\searrow$ 0.5 and that the process occurs without viscous-boundary-layer effects. For the remainder of this paper we shall focus on the lee vortices that appear in this low-Fr flow regime.

### b. *Comparison with laboratory experiments*

Although the extant relevant laboratory simulations use obstacles with $h \sim L$, have a no-slip lower surface, and have reflective upper boundary conditions, some of the features are so strikingly similar to the present results that we thought it worthwhile to note them here.

Figure 4 displays a close-up view of the flow on the center plane and surface in the experiment with Fr = 0.22 (Figs. 1c and 3c). This flow is in qualitative agreement with that shown in Fig. 15a of the laboratory